J. Phys. B: At. Mol. Opt. Phys. 28 (1995) 2425-2433. Printed in the UK

Photoabsorption study of ligand-field splitting of Br-3d levels in HBr

R Püttner, M Domke, K Schulz, A Gutiérrez and G Kaindl

Institut für Experimentalphysik, Freie Universität Berlin Arnimallee 14, D-14195 Berlin-Dahlem, Germany

Received 17 February 1995

Abstract. The inner-shell photoabsorption spectrum of gas-phase HBr below the Br-3d ionization thresholds was measured with high spectral resolution. Ligand-field splitting of the Br-3d levels could be clearly resolved in photoabsorption, in agreement with observations made in recent photoemission work. The good signal-to-noise ratio of the present photoabsorption spectrum allowed to follow the ligand-field splitting of 3d-core-excited np Rydberg states up to high quantum numbers ($n=9$), and to assign some additional weak transitions that could not be resolved before.

1. Introduction

During recent years, the energy resolution of extreme-ultraviolet (XUV) and soft-x-ray monochromators at synchrotron-radiation facilities has been considerably improved, leading to substantial progress in the study of inner-shell excitations in atoms and molecules. It has now become possible to resolve vibrational splittings and ligand-field splittings in a number of core-excited molecules [1]. Ligand-field splitting of Xe-4d orbitals in XeF_2 and XeF_4 [2] as well as of shallow levels of the elements Zn, Ga, Pb, Cd, and Sn in gas-phase compounds or in form of metals [3–6] have been known since about two decades. Recently, ligand-field splitting of the S-$2p_{3/2}$ level (at $\simeq$170 eV) could be resolved for H_2S and D_2S in photoabsorption (PA) and in photoemission (PE) [7, 8] as well as of the I-4d and Br-3d levels, respectively, in PE for a number of iodine compounds [9–11] and for HBr [12]. Even though the observed ligand-field splittings were found to be as large as a few hundred meV, it is generally more difficult to identify them in PA than in PE, due to overlapping Rydberg series in the former case. In the present paper we focus on ligand-field splitting effects on the inner-shell photoabsorption spectrum of HBr.

A series of Rydberg states in the inner-shell PA spectrum of HBr had first been recorded by Shaw *et al* [13] employing high-resolution electron-energy-loss spectroscopy (EELS). In this early paper, ligand-field splitting was neglected and the existence of only two ionization thresholds ($3d_{5/2}$ and $3d_{3/2}$) was considered, leading to a number of inconsistencies between the data and the proposed assignments. For example, the splitting observed for the $(3d_{5/2})^{-1}5s\sigma$ resonance signal could not be explained. Recently, Liu *et al* reported the 3d core-level PE spectrum of HBr [12], revealing a ligand-field

0953-4075/95/122425+09$19.50

splitting of the 3d core level. Based on this observation as well as on the results of scattered-wave $X\alpha$ (sw-$X\alpha$) calculations, these authors re-assigned the EELS spectrum of Shaw *et al*. However, only the most intense structures ($4d\pi$, $5p\sigma$, $5p\pi$) could be identified due to the moderate signal-to-noise ratio of the early EELS spectrum.

In the present paper, we report on a high-resolution PA study of HBr in the region below the Br-$M_{4,5}$ thresholds at energies between 77 and 78 eV. The measurements were performed with better energy resolution ($\leqslant 10$ meV) and substantially better signal-to-noise ratio than in previous studies. The experimental improvements allowed us to assign the Rydberg states up to high quantum numbers n (up to 9p), and to separate the observed spectrum into states that converge towards five different ionization thresholds caused by ligand-field splitting. Moreover, we were able to assign several weak structures that had not been observed before.

2. Experimental and data analysis

The measurements were performed with the high-resolution plane-grating SX700/II monochromator, which is operated by the Freie Universität Berlin at the Berliner Elektronenspeicherring für Synchrotronstrahlung (BESSY) [14]. Using a 2442 lines/mm grating, a resolution of slightly better than 10 meV (FWHM) was obtained in the energy region of the Br-$M_{4,5}$ thresholds, which is small compared to the intrinsic lifetime widths of the Br-3d excitations in HBr ($\simeq 95$ meV [13]; see also further below). The absolute energy scale was calibrated by comparison with the energy of the $v''=0 \rightarrow v'=0$ vibrational transition of the N $1s^{-1}\pi^*$ resonance in N_2 at 400.88 eV [15]. Photoabsorption spectra were measured with the use of an ionization cell that was separated from the ultra-high vacuum (UHV) by an $\simeq 1000$ Å thick carbon window [14]; the total photoionization current was measured as a function of photon energy. Typical pressures in the gas cell were in the 100 μbar range. The data were taken from high-purity HBr gas (99.8%) obtained from Messer-Griesheim, which was introduced into the gas cell without further purification. In the least-squares fit analyses of the spectra, the resonances were described by Voigt profiles, i.e. Lorentzians convoluted by a Gaussian to simulate the spectrometer function. The spectrometer function, however, is not a pure Gaussian, but has a weak non-Gaussian part with a Lorentzian component [14]. This has the consequence that the fitted intrinsic Lorentzian widths contain also a possible Lorentzian component of the spectrometer function and ought to be considered, therefore, as upper limits of the actual intrinsic Lorentzian widths. Since the well-resolved resonance lines turned out to have, on the average, intrinsic linewidths of $\simeq 95$ meV, with only small variations by up to $\simeq 7$ meV, we assumed intrinsic widths of the same magnitude for the less well-resolved or very weak resonances.

3. Photoionization spectrum below the $M_{4,5}$ thresholds

An overview photoabsorption spectrum of HBr in the region of the Rydberg excitations below the $M_{4,5}$ thresholds is shown in figure 1. In addition to the long-lived Rydberg resonances at energies above 73.5 eV, the spectrum exhibits a broad feature centred at $\simeq 71.3$ eV, which originates from a $(3d)^{-1}\sigma^*$ excitation. The linewidth of this σ-resonance is $\simeq 2.5$ eV (FWHM), which is by far too wide to allow spin–orbit or ligand-field splittings to be resolved. The situation is different in case of the rather narrow Rydberg

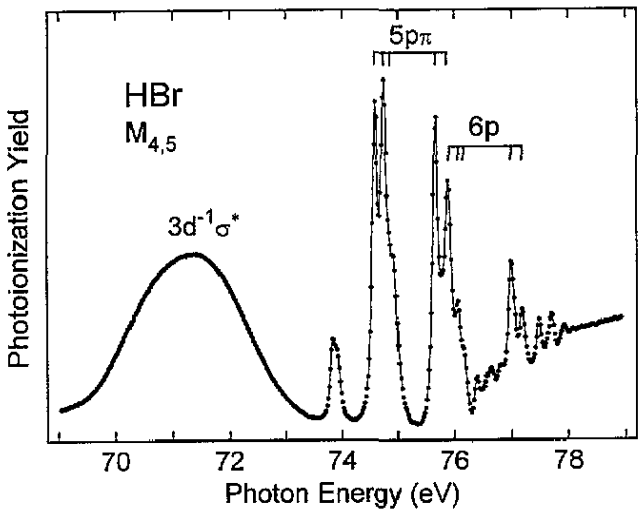

Figure 1. Overview of the Br-3d photoionization spectrum of HBr. Note the broad valence-state peak at $\simeq$71.3 eV and the narrow Rydberg states above $\simeq$73.5 eV. The ligand-field splittings of the 5pπ and 6p states are indicated by the vertical-bar diagrams.

resonances above $\simeq$73.5 eV, where such splittings can be clearly identified. As discussed further below, the 5pπ and 6p Rydberg states, e.g. split into five different substates due to spin–orbit and ligand-field splitting. For these two examples, the five resonance lines are marked by the vertical-bar diagrams in figure 1. The first three lines are due to ligand-field splitting of the Br-3$d_{5/2}$ (M_5) level, and the last two are caused by ligand-field splitting of the Br-3$d_{3/2}$ (M_4) level. We would like to point out that almost every Rydberg state is seen five-fold in the present spectrum, with the exception of the very weak or partly forbidden transitions.

The photoionization spectrum in the region of the Rydberg resonances is shown in more detail in figure 2. In order to arrive at the given assignments of the Rydberg series, we assumed five series converging towards five different thresholds. This assumption is in full agreement with the results of Liu *et al* [12] for the ligand-field splitting of the $M_{4,5}$ thresholds, i.e. three thresholds with $\Delta_{5/2}$, $\Pi_{3/2}$ and $\Sigma_{1/2}$ symmetry at M_5, and two thresholds with $\Delta_{3/2}$ and $\Pi_{1/2}$ symmetry at M_4. It should be emphasized here that no reasonable assignment of the observed resonance lines can be found with less than five thresholds. For the given assignments, we used the Rydberg formula $E = I_p - \mathrm{Ry}/(n-\delta)^2$ (I_p = ionization threshold; Ry = 13.605 eV), and assumed the quantum defects, δ, of the p and d series to be of similar magnitude as those known for the analogous Rydberg series in the isoelectronic atom Kr: $\delta_{p,Kr} \simeq 2.7$ and $\delta_{d,Kr} \simeq 1.3$ [16]; for the f series, the δ value was assumed to be much smaller. The Rydberg states are designated by $n\ell\lambda$, where n represents the principle quantum number, ℓ the dominant angular-momentum character of the orbital in the outer sphere of the molecule, and λ the symmetry along the molecular axis; the latter is equal to the angular momentum parallel to the molecular axis, L_z. Note that this designation bears in mind a further symmetry splitting of all orbitals with $\ell \neq 0$, e.g. a p Rydberg state can split into pσ and pπ. Such a splitting is caused by the different penetration of the orbitals into the 'molecular core' created by both the H and the Br atom. In case of pσ, the orbital is mainly parallel to the molecular axis and the penetration is stronger than in case of pπ. This leads to the binding energy of the pσ orbital to be slightly higher than that

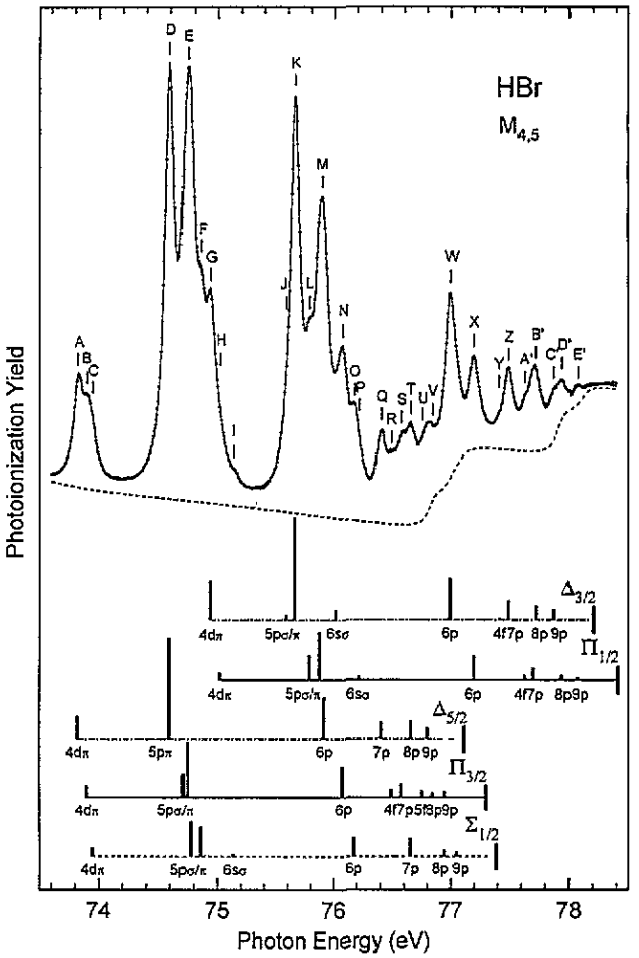

Figure 2. High-resolution photoionization spectrum of HBr in the region of the Rydberg resonances below the $M_{4,5}$ ionization thresholds. The solid curve through the data points represents the result of a least-squares fit with five Rydberg series converging to five different ionization thresholds ($\Delta_{3/2}$, $\Pi_{1/2}$, $\Delta_{5/2}$, $\Pi_{3/2}$, $\Sigma_{1/2}$), split by spin-orbit and ligand-field interaction. The energies and relative intensities of the individual resonance lines are represented by the five vertical-bar diagrams, with the lengths of the bars being proportional to the intensities. The dashed curve below the spectrum represents the integral background.

of the pπ orbital. With increasing quantum number n, the orbitals become increasingly more extended, and the differences in penetration can be neglected. Hence, the symmetry splitting of p orbitals into pσ and pπ can only be observed for orbitals with small n. The quantum number λ was consequently neglected in the assignments for the higher n Rydberg states. The situation in a molecule leads to transition rules different from those in an atom. Since, e.g. in our designation, the 4d orbital has mainly d character in the outer sphere, but may also possess some p character at the Br site, a 3d→4d transition can be possible. However, the allowed resonances are those complying with the selection rules for electronic transitions, i.e. $\Delta\lambda = 0, \pm 1$, allowing no spin flip. Consequently, transitions like 3d$\sigma \rightarrow n\ell\delta$ or 3d$\delta \rightarrow n\ell\sigma$ are forbidden and are expected to have zero intensities.

We also made use of the results of the sw-$X\alpha$ calculations [12] for the relative intensities as well as the orbital order of the Rydberg resonances. Our designation of Rydberg orbitals, $n\ell\lambda$, is well suited for assigning Rydberg states. It is, however, different from the nomenclature for molecular orbitals used in the sw-$X\alpha$ calculations. Since the results of these calculations will be used in the following, we briefly compare the two designations. Let us consider, e.g. the 11σ orbital of the sw-$X\alpha$ calculation, which has a strong p character in its charge distribution; it is therefore designated as a p orbital. Due to its molecular σ symmetry it can also be designated as $5p\sigma$. The 6π orbital has a strong p character in its charge distribution, too [12]. Its molecular symmetry is π and it is hence designated as $5p\pi$. In this way we arrive at the following orbitals and their calculated oscillator strengths (designations and oscillator strengths are from [12]): $5s\sigma$ (11σ; 0.0003), $4d\pi$ (5π; 0.0039), $4d\delta$ (2δ; 0.0000), $5p\sigma$ (11σ; 0.0029), $5p\pi$ (6π; 0.0091), $6s\sigma$ (12σ; 0.0014).

4. Detailed assignment of resonance lines

Positions and relative intensities of the resonances of the Rydberg series converging towards the five different thresholds are represented by the five bar diagrams in figure 2. The dashed curve under the spectrum represents the integral background. The solid curve through the data points in figure 2 represents the result of the described least-squares fit analysis. Note that the ligand-field splittings can be clearly identified. As in the core-excitation spectrum of Kr, the resonances of the p series, converging towards the various thresholds, are also most intense in the spectrum of HBr [14, 16]. With the energies of the p resonances and the Rydberg formula, the energies of the five thresholds, I_p, were calculated; they are given in table 1, where they are also compared with the results of Liu *et al* [12]. Our values for the threshold energies, if shifted to higher energies by $\simeq 35$ meV, are in good agreement with those of [12]. Only the $\Sigma_{1/2}$ threshold energy exhibits a slightly larger deviation to lower energies. This can be due to a larger error bar for this threshold in the PE measurements, since the $\Sigma_{1/2}$ threshold leads only to a weak shoulder in the $3d_{5/2}$ core-level PE peak of HBr. Since no calibration of the energy scale was reported in [12], we believe that the present threshold energies ought to be preferred. Table 2 summarizes the energies and quantum defects, δ, for each resonance as obtained from the spectrum reproduced in figure 2.

The peak at $\simeq 73.9$ eV consists of three resonances (peaks A, B, C). A description of this structure by only two resonances can be excluded, since the resonance at 73.824 eV (peak A) has a width of no more than 95 meV, and—assuming only two resonances—the linewidth of its high-energy shoulder would become much broader

Table 1. Energies of the five ionization thresholds caused by spin–orbit and ligand-field splitting of the Br-3d core-excited state in HBr.

	Threshold energy I_p (eV)	
Symbol	This work	Liu *et al* [12]
$\Delta_{5/2}$	77.114 (10)	77.15
$\Pi_{3/2}$	77.301 (10)	77.34
$\Sigma_{1/2}$	77.390 (10)	77.46
$\Delta_{3/2}$	78.206 (10)	78.24
$\Pi_{1/2}$	78.415 (10)	78.45

Table 2. Resonances and their assignments in the high-resolution photoionization spectrum of HBr. The quoted values for energy E and quantum defect δ result from the least-squares fit analysis of the spectrum in figure 2. The numbers in parentheses are the error bars in units of the last digit.

		Excitation					
Peak	E (eV)	$(3d\delta_{5/2})^{-1}$	$(3d\pi_{3/2})^{-1}$	$(3d\sigma_{1/2})^{-1}$	$(3d\delta_{3/2})^{-1}$	$(3d\pi_{1/2})^{-1}$	δ
A	73.824 (5)	4dπ					1.97
B	73.897 (10)		4dπ				2.00
C	73.944 (10)			4dπ			2.01
D	74.590 (3)	5pπ					2.68
E	74.710 (30)		5pσ				2.71
E	74.744 (10)		5pπ				2.69
E	74.772 (10)			5pσ			2.72
F	74.857 (10)			5pπ			2.68
G	74.938 (5)				4dπ		1.96
H	75.015 (10)					4dπ	2.00
I	75.136 (10)			6sσ			3.54
J	75.584 (10)				5pσ		2.73
K	75.661 (3)				5pπ		2.69
L	75.784 (10)					5pσ	2.72
M	75.875 (10)					5pπ	2.69
M	75.915 (10)	6p					2.64
N	76.016 (10)				6sσ		3.51
N	76.075 (10)		6p				2.67
O	76.177 (10)			6p			2.65
P	76.215 (10)					6sσ	3.51
Q	76.399 (10)	7p					2.64
R	76.488 (10)		4f				−0.1
S	76.574 (10)		7p				2.67
T	76.655 (10)	8p		7p			2.70/2.56
U	76.752 (10)		5f				0
V	76.797 (10)	9p					2.48
V	76.842 (10)		8p				2.62
	76.946 (10)		9p	8p			2.72/2.40
W	76.993 (5)				6p		2.65
	77.052 (10)			9p			2.66
X	77.196 (5)					6p	2.65
Y	77.413 (10)				4f		−0.14
Z	77.489 (10)				7p		2.64
A′	77.628 (10)					4f	−0.15
B′	77.699 (10)					7p	2.67
C′	77.724 (10)				8p		2.69
C′	77.873 (10)				9p		2.61
D′	77.940 (10)					8p	2.65
E′	78.073 (10)					9p	2.69

than 95 meV. According to the results of the sw-$X\alpha$ calculations, these three resonances ought to be assigned to $(3d\delta_{5/2})^{-1}4d\pi$, $(3d\pi_{3/2})^{-1}4d\pi$ and $(3d\sigma_{1/2})^{-1}4d\pi$ excitations, respectively. Note that in these designations, the greek symbol characterizes the symmetry of the core hole: Rydberg series with excitations from a 3d state with $\delta_{5/2}$, $\pi_{3/2}$, $\sigma_{1/2}$, $\delta_{3/2}$ and $\pi_{1/2}$ symmetry converge towards the $\Delta_{5/2}$, $\Pi_{3/2}$, $\Sigma_{1/2}$, $\Delta_{3/2}$ and $\Pi_{1/2}$ ionization thresholds, respectively. An alternative assignment to 5sσ or 4dδ states is unlikely because of the calculated oscillator strengths as well as the selection rules,

which actually forbid $(3d\delta)^{-1}n\ell\sigma$ and $(3d\sigma)^{-1}n\ell\delta$ excitations; also, only two resonances would be expected in this case, in contrast to our observation.

The ligand-field splittings of the $4d\pi$ peaks in the three Rydberg series converging towards the $\Delta_{5/2}$, $\Pi_{3/2}$ and $\Sigma_{1/2}$ thresholds are smaller than those of the corresponding thresholds (see also tables 1 and 2). Hence, it must be concluded that the term values for the $4d\pi$ orbitals depend on the orientation of the created 3d hole relative to the molecular axis. We assume that this leads to a variation of the Coulomb interaction between the $4d\pi$ Rydberg electron and H. In fact, the term value increases from Δ to Σ. Screening of the core hole is influenced by the orientation of the hole relative to the molecular axis of HBr. In case of a Σ hole (a $(3d\sigma)^{-1}n\ell\lambda$ excitation), which is oriented along the axis of HBr, screening is stronger by σ valence electrons, which remove electronic charge from the H atom. As a consequence, the H atom would feel a stronger Coulomb interaction with the excited $4d\pi$ electron, reducing the $(3d\sigma_{1/2})^{-1}$ $4d\pi$ excitation energy as compared to a Δ or Π hole. Due to Coulomb interaction and the fast increase of $\langle r\rangle$ for electrons in higher Rydberg orbitals, the interaction becomes increasingly weaker with increasing n. Assuming the Coulomb interaction between the excited orbital and the H atom (and consequently the energy shift) to be independent from spin–orbit interaction, we assign the peaks at 74.938 eV (peak G) and at 75.015 eV (peak H) to $(3d\delta_{3/2})^{-1}4d\pi$ and to $(3d\pi_{1/2})^{-1}4d\pi$ excitations, respectively.

We now consider the 5p and the 6p Rydberg states; here, only the 5p states are split into $5p\sigma$ and $5p\pi$ orbitals. In agreement with calculations [12], $5p\sigma$ has a slightly higher binding energy than $5p\pi$. The strong resonance at 74.590 eV (peak D) is assigned to $(3d\delta_{5/2})^{-1}5p\pi$, in agreement with the results of the sw-$X\alpha$ calculations, which predict a stronger oscillator strength for $5p\pi$ than for $5p\sigma$. The $3d\delta_{5/2}\rightarrow 5p\sigma$ transition is forbidden, as mentioned before. The next structure at $\simeq$74.75 eV (peak E) contains more than one excitation. This becomes evident when we consider the relative intensities of excitations to higher np orbitals, as e.g. to the 6p orbitals, which belong to the five different ionization thresholds. The 6p resonances are well resolved and their relative intensities can therefore readily be determined. The only exception is peak M at $\simeq$75.895 eV, which is composed of the two components $(3d\pi_{1/2})^{-1}5p\pi$ and $(3d\delta_{5/2})^{-1}6p$. The contribution of the 6p resonance to peak M can be estimated on the basis of the intensity ratio of the $(3d\delta_{3/2})^{-1}6p$ and $(3d\pi_{1/2})^{-1}6p$ excitations, and the assumption that the intensity ratio of the $(3d\delta_{3/2})^{-1}5p\sigma/\pi$ [sum of intensities of the $(3d\delta_{3/2})^{-1}5p\sigma$ and the $(3d\delta_{3/2})^{-1}5p\pi$ excitation] to the $(3d\pi_{1/2})^{-1}5p\sigma/\pi$ excitations is of equal size. This assumption seems to be justified, since the intensity ratios of the analogous excitations to np states ($n=6$ to 9) are found to be equal. An analogous consideration for the sum of intensities of the $5p\sigma$ and $5p\pi$ Rydberg states converging towards the five different thresholds shows that peak E at $\simeq$74.75 eV is too intense to be composed of only the two components $(3d\pi_{3/2})^{-1}5p\sigma$ and $(3d\pi_{3/2})^{-1}5p\pi$. In fact, a third component, $(3d\sigma_{1/2})^{-1}5p\sigma$, has to be taken into account. Then, the excitation energies of the three resonances composing peak E are determined as 74.710 eV $[(3d\pi_{3/2})^{-1}5p\sigma]$, 74.744 eV $[(3d\pi_{3/2})^{-1}5p\pi]$ and 74.772 eV $[(3d\sigma_{1/2})^{-1}5p\sigma]$.

The resonances at 75.661 eV (peak K), at 75.784 eV (peak L) and at 75.875 eV (low-energy part of peak M) are assigned to $(3d\delta_{3/2})^{-1}5p\pi$, $(3d\pi_{1/2})^{-1}5p\sigma$ and $(3d\pi_{1/2})^{-1}5p\pi$ excitations, respectively. The weak low-energy shoulder of peak K at 75.584 eV (peak J) is assumed to stem from a $(3d\delta_{3/2})^{-1}5p\sigma$ excitation. This latter resonance is forbidden on the basis of selection rules for electronic transitions, since $\Delta\lambda=2$, but it will be allowed ($\Delta J_z=1$) if we assume a spin flip.

In the Rydberg series converging towards the $\Sigma_{1/2}$, $\Delta_{3/2}$ and $\Pi_{1/2}$ ionization thresholds, the $5p\sigma/\pi$ symmetry splitting amounts to $\simeq$85 meV; in case of the Rydberg

series converging towards the $\Pi_{3/2}$ ionization threshold, the least-squares fit reveals a symmetry splitting of only $\simeq$35 meV. However, in the energy region of peak *E* the fitted energies and intensities are not unambiguous, i.e. the 35 meV symmetry splitting has to be considered as preliminary.

Apart from the five *n*p Rydberg series, which were found to be split into *n*pσ and *n*pπ states, weak shoulders were observed. These shoulders at 75.136 eV (peak I), 76.016 eV (part of peak N) and 76.215 eV (peak P) can be assigned to $(3d\sigma_{1/2})^{-1}6s\sigma$, $(3d\delta_{3/2})^{-1}6s\sigma$ and $(3d\pi_{1/2})^{-1}6s\sigma$ excitations, respectively, taking the results of the sw-$X\alpha$ calculations into account [12]. The $(3d\delta_{5/2})^{-1}6s\sigma$ excitation is forbidden on the basis of selection rules, and a $(3d\pi_{3/2})^{-1}6s\sigma$ signal is likely to be present in the trailing edge of the $(3d\pi_{1/2})^{-1}4d\pi$ resonance (peak H). It would also be possible to assign the shoulder at 75.136 eV (peak I) to a $(3d\delta_{3/2})^{-1}4d\delta$ or $(3d\pi_{1/2})^{-1}4d\delta$ excitation, resulting in reasonable quantum defects of $\delta_d = 1.89$ or $\delta_d = 1.96$ (see further below). However, the calculated oscillator strength for the $3d\rightarrow 4d\delta$ transition is predicted to be zero [12]; we are therefore convinced that the former assignment of peak I is more likely. It might appear surprising that one observes a 6sσ but not a 5sσ signal. However, the oscillator strength of the 6sσ excitation was calculated to be five times higher than that of the 5sσ excitation, a phenomenon that is probably due to the stronger Br-p character of 6sσ as compared to 5pσ [12].

Additional transitions can be identified, particularly beyond the M_5 thresholds; e.g. the shoulder at 77.628 eV (peak A') is too intense to be assigned to a high-*n*s or -*n*d state. It cannot be a p state as well, since the p series can be clearly identified in this energy range. Therefore, we assign peak A' to a $(3d\pi_{1/2})^{-1}4f$ excitation, with a term value of 0.784 eV and a quantum defect of $\delta = -0.15$. Additionally, f states with $\delta \simeq -0.1$ can be identified at 76.488 eV (peak R), 76.752 eV (peak U) and 77.413 eV (peak Y); they are assigned to $(3d\pi_{3/2})^{-1}4f$ resonances, $(3d\pi_{3/2})^{-1}5f$ and $(3d\delta_{3/2})^{-1}4f$ resonances, respectively. A further f state, $(3d\sigma_{1/2})^{-1}4f$, is expected to lie at $\simeq$76.575 eV [at the position of the $(3d\pi_{3/2})^{-1}7p$ state (peak S)]; however, it cannot be resolved. The transition $3d\delta_{5/2}\rightarrow 4f$ is expected to occur at $\simeq$76.330 eV, but it is missing in the present spectrum. It can be also seen that the $(3d\pi_{1/2})^{-1}4f$ excitation is much more intense than the $(3d\delta_{3/2})^{-1}4f$ resonance. These two observations are analogous to the intensities of the 5pσ Rydberg states, and can be explained on the basis of the selection rules by assuming that the observed 4f state has σ symmetry. The quantum defects of the s, p, d and f series are determined to be 3.52, 2.66, 1.98 and -0.1, respectively. The value for the p series is similar to that found previously for the p series in isoelectronic Kr ($\delta_{Kr} \simeq 2.7$) [16], supporting the given assignments for the p series.

We would like to point out that all peaks in the present spectrum can be explained consistently on the basis of ligand-field splitting. In the PA spectrum of core-excited HBr, higher vibrational levels are obviously not excited. This becomes evident, when we consider the vibrational energy of the core-excited molecule ($h\nu_e \simeq 250$ meV), which was measured by PE [12]. Consequently, the first excited vibrational state ($v'' = 0 \rightarrow v' = 1$) of the resonance structure at $\simeq$73.9 eV is expected at $\simeq$74.15 eV, but no signal is observed at this energy. In addition, vibrational excitations in diatomic halide compounds, like HBr, HI, I_2, ICl and IBr, were found to be weak in core-level PE spectra [9, 12], and they have not been observed in inner-shell PA spectra of HCl and Cl_2 [13, 17, 18]. The missing of such vibrational sidebands in the core-excited spectra indicates a small change of the internuclear equilibrium distance upon inner-shell excitation from its ground-state value ($R_g = 1.414$ Å) [19].

5. Summary

In summary, the Br-3d photoabsorption spectrum of HBr was measured with high spectral resolution and good signal-to-noise ratio. This enabled us to assign Rydberg states up to high quantum numbers n, making use of calculated oscillator strengths as well as of the sequence of orbitals from recent sw-$X\alpha$ calculations [12]. Only orbitals with large calculated oscillator strengths ($4d\pi$, $5p\sigma$, $5p\pi$, $6s\sigma$) were identified, while those with small calculated oscillator strengths ($5s\sigma$, $4d\delta$) are missing. The PA spectrum exhibits resonance lines that converge towards five different ionization thresholds, which can be explained on the basis of ligand-field splitting of the core levels. This confirms the ligand-field splitting of the ionization thresholds observed in a recent PE study [12]. Ligand-field splitting can be analysed much easier in PE spectra as compared to PA: The values derived in a recent PE study [12] were very helpful in assigning the various resonances in the PA spectrum. Therefore, substantial progress in high-resolution PE would be quite useful for a better understanding of inner-shell PA spectra, particularly in cases, where several neighbouring thresholds occur.

Acknowledgments

This work was supported by the Bundesminister für Forschung und Technologie, project #05-5KEAXI-3/TP03. One of the authors (AG) thanks the Spanish Ministerio de Educación y Ciencia for financial support.

References

[1] See e.g. Sutherland D G J, Liu Z F, Bancroft G M and Tan K H 1994 *Nucl. Instrum. Methods* B **87** 183
[2] Comes F J, Haensel R, Nielsen U and Schwarz W H E 1973 *J. Chem. Phys.* **58** 516
[3] Bancroft G M, Coatsworth L L, Creber D K and Tse J 1977 *Chem. Phys. Lett.* **50** 228
[4] Bancroft G M and Creber D K 1977 *J. Chem. Phys.* **67** 4891
[5] Wertheim G K and Buchanan D N E 1989 *Solid State Commun.* **69** 689
[6] Bancroft G M, Bristow D J and Tse J S 1983 *Chem. Phys.* **75** 277
[7] Hudson E, Shirley D A, Domke M, Remmers G and Kaindl G 1994 *Phys. Rev.* A **49** 161
[8] Svensson S, Ausmees A, Osborne S J, Bray G, Gel'mukhanov F, Ågren H, Naves de Brito A, Sairanen O-P, Kivimäki A, Nõmmiste E, Aksela H and Aksela S 1994 *Phys. Rev. Lett.* **72** 3021
[9] Cutler J N, Bancroft G M and Tan K H 1992 *J. Chem. Phys.* **97** 7931
[10] Cutler J N, Bancroft G M, Sutherland D G and Tan K H 1991 *Phys. Rev. Lett.* **67** 1531
[11] Cutler J N, Bancroft G M and Tan K H 1991 *J. Phys. B: At. Mol. Opt. Phys.* **24** 4897
[12] Liu Z F, Bancroft G M, Tan K H and Schachter M 1994 *J. Electron. Spectrosc. Relat. Phenom.* **67** 299
[13] Shaw D A, Cvejanovic D, King G C and Read F H 1984 *J. Phys. B: At. Mol. Phys.* **17** 1173
[14] Domke M, Mandel T, Puschmann A, Xue C, Shirley D A, Kaindl G, Petersen H and Kuske P 1992 *Rev. Sci. Instrum.* **63** 80
[15] Sodhi R N S and Brion C E 1984 *J. Electron. Spectrosc. Relat. Phenom.* **34** 363
[16] King G C, Tronc M, Read F H and Bradford R C 1977 *J. Phys. B: At. Mol. Phys.* **10** 2479
[17] Ninomiya K, Ishiguro E, Iwata S, Mikuni A and Sasaki T 1981 *J. Phys. B: At. Mol. Phys.* **14** 1777
[18] Shaw D A, King G C and Read F H 1980 *J. Phys. B: At. Mol. Phys.* **13** L723
[19] Huber K B and Herzberg G 1979 *Molecular Spectra and Molecular Structure IV: Constants of Diatomic Molecules* (New York: Van Nostrand) p 278